Int J Thermophys (2010) 31:1739–1748
DOI 10.1007/s10765-010-0831-8

# Shell Perturbations of an Acoustic Thermometer Determined from Speed of Sound in Gas Mixtures

**R. M. Gavioso · D. Madonna Ripa · C. Guianvarc'h · G. Benedetto · P. A. Giuliano Albo · R. Cuccaro · L. Pitre · D. Truong**

Received: 29 May 2010 / Accepted: 16 September 2010 / Published online: 6 October 2010


**Abstract** With the goal of achieving a better understanding of gas–shell coupling perturbations in the acoustic resonators used at INRiM for the determination of the Boltzmann constant, we measured the variation of their acoustic and microwave resonances induced by changing the composition of a binary He–Ar mixture which filled the cavity at constant temperature and pressure. As a consequence of the progressive dilution of a sample of initially pure He with Ar, the radial acoustic modes of the resonator spanned decreasing frequency intervals, partially overlapping, for several modes. In addition to the expected breathing mode of the shell, the results evidenced the presence of several other shell resonances at lower and higher frequencies, confirming that the elastic response of the assembled resonator significantly differs from that of a simple spherical shell. Experimental results are reported for two resonators which differ in design, dimensions, and constructing material. In spite of their being preliminary and susceptible of significant improvement, these results favor the interpretation of acoustic thermometry measurements with pure gases.

**Keywords** Acoustic thermometry · Shell coupling · Speed of sound

## 1 Introduction

The effects of acoustic coupling between the shell and the gas filling an acoustic cavity have been theoretically investigated and modeled previously [1] on the basis of the

R. M. Gavioso (✉) · D. Madonna Ripa · C. Guianvarc'h · G. Benedetto · P. A. Giuliano Albo · R. Cuccaro
Thermodynamics Division, Istituto Nazionale di Ricerca Metrologica, 10135 Turin, Italy
e-mail: r.gavioso@inrim.it

L. Pitre · D. Truong
Laboratoire Commun de Métrologie LNE-CNAM, La Plaine-Saint-Denis, France

exact theory of elasticity of isotropic materials. Though this model was routinely used to correct shell perturbations in several acoustic thermometry experiments [2,3], its overall performance may not be sufficient to the goal of reducing the uncertainty of an acoustic determination of the Boltzmann constant $k_B$ [4] at the target level of 1 part in $10^6$ or below. Particularly, the rather complicated mechanical structure formed by the acoustic resonator, the containing vessel, and their coupling system differs significantly from an isotropic spherical shell, limiting the validity of some assumptions of the analytical model. It was previously suggested that in real experimental conditions the radial acoustic modes may also efficiently couple to the non-radial elastic modes within the shell if the radial symmetry is broken, either by some deviation from sphericity of the detailed shape of the resonator or by a support [5]. Also, there is experimental evidence that the energy losses associated with efficient gas–shell coupling perturbations are more relevant than those predictable with the model in [1], in spite of its inclusion of mechanisms such as the acoustic radiation from the outer cavity surface. Different modeling and experimental strategies have been proposed and worked out to overcome the limits discussed above. Due to the complexity of an analytical calculation capable of accounting for more realistic boundary conditions, modeling efforts have so far concentrated on finite-element methods (FEM) [6,7]. For one of the resonators previously used at INRiM, two-dimensional FEM calculations have shown that the combined effect of the shape defects and the supporting structure raises the shell eigenfrequencies with respect to the corresponding modes of the isolated uniform shell [6].

With regard to experimental techniques, the mechanical response of the shell has been excited using a modal impact hammer and detected using accelerometers [8]. In a previous variant of the same method, piezoelectric excitation and detection were used [9]. In both these experiments the shell response was found to depend on the relative position of the exciter and the detector and the identification of the shell modes by comparison with their expected frequency was not straightforward.

Alternatively, the speed of sound in the gas filling the cavity may be varied, and the coupling effects directly revealed by continuous recording of the acoustic resonances within the cavity. Importantly, this procedure determines the perturbing effects directly and does not strictly imply the identification of the shell modes, or the development of a model to account for their perturbing effect. This method was first applied using a temperature variation to produce the necessary change in the speed of sound [2,9]. In this study, we suggest an alternative method based on the same basic principle. Here, the variation of speed of sound is caused by a change of the composition of a binary He–Ar mixture. Among the advantages of this method we note: the arbitrary choice of the working temperature and pressure during the experiment; the possible exploration of a wider frequency range, with arbitrary resolution; and the exploration of the same frequency range with more than a single mode, allowing a check for the repeatability of perturbing effects on modes of different order. These peculiar features simplify the identification of shell perturbations from those related to other physical effects.

Though the study and results presented here are still preliminary, they have already proven their usefulness in improving the comprehension of the observed perturbations of an acoustic resonator.

## 2 Experiment and Method

In this study, we report acoustic results obtained with the two cavities sketched in Fig. 1: (i) a spherical steel resonator (INRiM1) with a inner radius of 60 mm and wall thickness of 12.8 mm and (ii) a triaxial ellipsoid copper resonator (TCU2v2) designed and realized at LNE-CNAM. The internal geometry of TCU2v2 is defined by three slightly different orthogonal axes: $a$, $a(1+\varepsilon_1)$, and $a(1+\varepsilon_2)$ with $a = 50\,\text{mm}$, $\varepsilon_1 = 1.2 \times 10^{-3}$, $\varepsilon_2 = 0.8 \times 10^{-3}$, and an average wall thickness of 10 mm. For the most part, the instrumentation and the procedures used for the determination of acoustic and microwave measurements were unchanged from those routinely used in acoustic thermometry and described elsewhere [10]. In its preliminary realization, the procedure adopted to progressively dilute a sample of initially pure helium simply consisted of repeated injections of argon, raising the value of the static pressure above the set point, followed by repeated pressure reductions of equal amounts. As a major drawback of this procedure, the time required for re-equilibration after each pressure variation was impractically long. Thus, the acoustic resonances were recorded and fitted while still decreasing as a function of time with relative rates up to $50\,\text{ppm} \cdot \text{min}^{-1}$. These shifts limited the fitting precision and the number of investigated modes. On the basis of this experience, the procedure for the acquisition of TCU2v2 data was changed by realizing the simple manifold schematized in Fig. 2. Here, the inlet flow to the resonator is regulated by two mass-flow controllers (MFCs) connected to He and Ar sampling bottles. The MFCs set points can be varied to adjust the desired composition of the mixture within the resolution of their controlling units, determined as $1 \times 10^{-3}$ of their full-scale range (100 sccm, or $0.17\,\text{m}^3 \cdot \text{Pa} \cdot \text{s}^{-1}$), which corresponds to a resolution of around 300 ppm in the He molar fraction $x$. A solenoid valve (f.s. range 100 sccm) regulates the outlet flow through an evacuating line connected to the vessel.

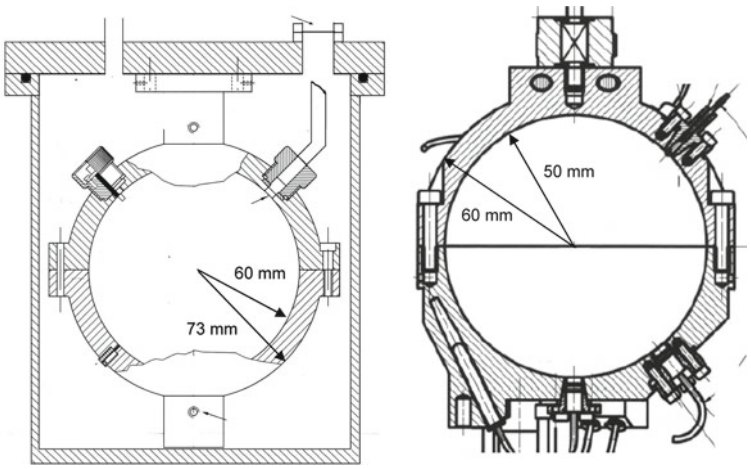


**Fig. 1** Cutaway sketch of the acoustic cavities used in this work: (*left*) stainless steel spherical resonator INRiM1; (*right*) triaxial ellipsoid copper resonator TCU2v2. In operation both resonators were bolted to the lid of a cylindrical stainless steel vessel

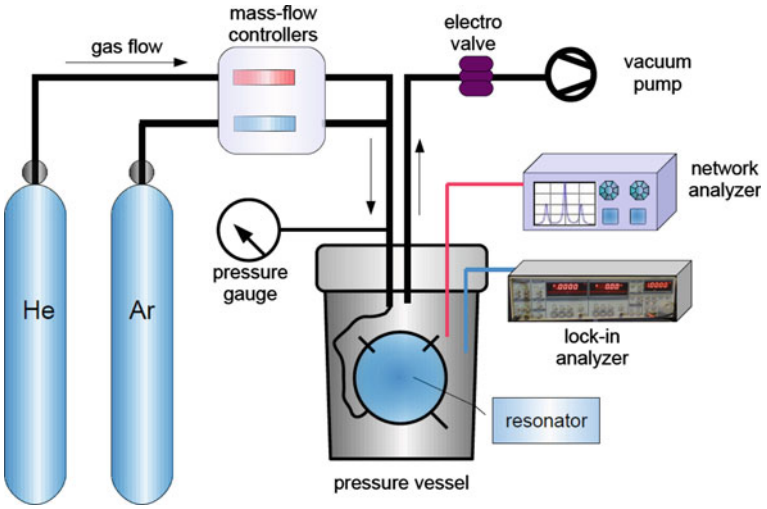


**Fig. 2** Schematic diagram of the manifold and instrumentation used to flow a mixture of variable composition through an acoustic resonator at constant temperature and pressure

This regulation maintains the pressure in the resonator constant within $\pm 1$ Pa of the set point. The sequence of the set points for the two MFCs is simulated to fulfill the resolution requirements in the successive variations of the mixture composition and to correspond to an approximately linear variation of the sound speed. At every change in the relative flow of the MFCs, diffusion and replacement of the gas contained within the cavity require a transitory time to elapse before the achievement of stable thermodynamic conditions. These variations were rapidly tracked as a function of time by an automated procedure phase-locked on the acoustic resonance frequency of a single mode. Finally, when preset stability conditions were reached, the acoustic resonances of several acoustic modes of interest were scanned and fitted. With this procedure, the acquisition of a data set of about 800 different molar fractions in the range $1 > x > 0$ required about 6 weeks of acquisition time.

At each different composition, $x$ was determined from a microwave analysis as the only meaningful solution of the equation,

$$\frac{\varepsilon_{\rm mix} - 1}{\varepsilon_{\rm mix} + 2} = \rho_0 \frac{1}{(1 + B_{\rm mix}\rho_0)} [x A_{\rm He} + (1 - x) A_{\rm Ar}] \tag{1}$$

where $(1-x)$ is the molar fraction of Ar, $\rho_0$ is the ideal gas density, $A_i$'s are the molar polarizabilities at zero density, and $B_{\rm mix} = x^2 B_{\rm He} + 2x(1-x) B_{\rm He-Ar} + (1-x)^2 B_{\rm Ar}$ is the second density virial coefficient of the mixture. The mixture permittivity $\varepsilon_{\rm mix}$ is obtained from that of pure helium $\varepsilon_{\rm He}$ and the squared ratios of the average resonance frequencies $f_{\rm TM11}$ of the microwave mode TM11 as

$$\varepsilon_{\rm mix} = \varepsilon_{\rm He} \left( \frac{\langle f_{\rm TM11} \rangle_{\rm He}}{\langle f_{\rm TM11} \rangle_{\rm mix}} \right)^2 . \tag{2}$$

All the thermodynamic and electric properties of He and Ar that are needed to solve Eq. 2 are accurately known from experiment or calculation [11–13].

## 3 Analysis and Discussion of Acoustic Results

Acoustic data were recorded at 800 kPa, 273.16 K for five purely radial modes (0,2) to (0,6) of INRiM1, while the composition of the He–Ar mixture filling the cavity was slowly varied between $1 > x > 0.5$. For TCU2v2, six radial modes were investigated, namely, (0,2) to (0,8), with the exception of (0,7) for reason of its strong and variable overlapping with a non-radial neighboring mode in the acoustic spectrum which prejudiced the successful identification and location of this mode from the automated software. For the same reason and to speed up the acquisition procedure, the measurement for radial modes of higher order was not carried out. Measurements for TCU2v2 took place at 690 kPa, 273.16 K. This particular choice of the working pressure was imposed by the full-scale range of the employed pressure transducer.

**Table 1** Selected mechanical and elastic properties of copper and steel relevant to the calculation of the shell admittance

| Notation | Property (unit) | Copper [16] | 316 Stainless steel [10] |
|---|---|---|---|
| $\rho_{sh}$ | Shell density ($kg \cdot m^{-3}$) | 8940 | 7900 |
| $Y$ | Young's modulus (GPa) | 127 | 197 |
| $\sigma$ | Poisson's ratio | 0.344 | 0.293 |
| $u_{sh} = \sqrt{\frac{Y}{\rho_{sh}} \frac{(1-\sigma)}{(1-2\sigma)(1+\sigma)}}$ | Longitudinal speed of sound in the shell ($m \cdot s^{-1}$) | 4714 | 5784 |

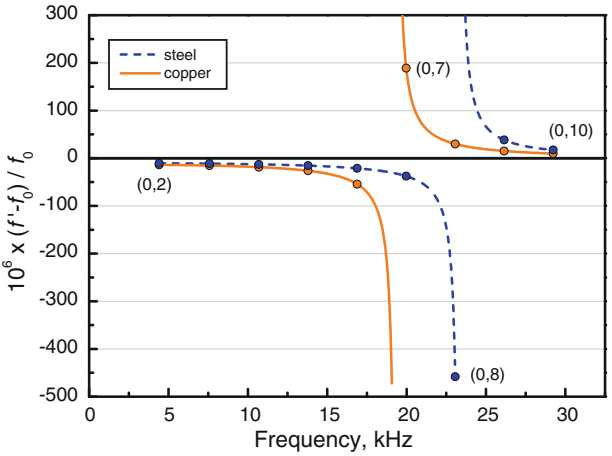


**Fig. 3** Comparison of the relative shell perturbations $\Delta f'_{shell} = (f' - f_0)/f_0$ to the radial acoustic modes (0,2) to (0,10) for a 5 cm inner radius spherical shell (realized in steel or copper) filled with Ar at 690 kPa

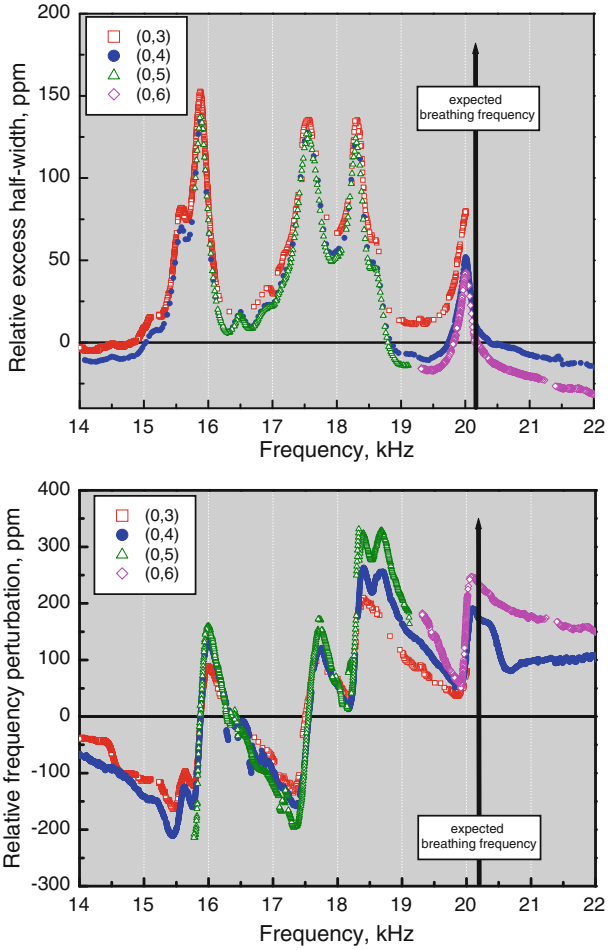


**Fig. 4** Relative excess halfwidths and frequency perturbations of radial modes recorded for the resonator INRiM1. The curves for different modes, respectively, correspond to the compositions: $0.51 < x_{(0,3)} < 0.88$; $0.66 < x_{(0,4)} < 0.93$; $0.51 < x_{(0,5)} < 0.71$; $0.51 < x_{(0,6)} < 0.65$, where $x_{(0,n)}$ is the molar fraction of He in the mixture while recording the resonance frequency of mode $(0, n)$

To prepare the acoustic data for the investigation of shell perturbations, we corrected the experimental frequencies $f_{0n}$ (the subscript index identifies the $n$th radial mode) for all known perturbing effects [10]. These included boundary layer effects, the presence of ducts and microphones and geometrical corrections (TCU2v2 only). Simple weighting mixing rules were applied to estimate the thermodynamic properties of the mixture which are needed for these calculations. However, the calculation of the predominant boundary layer perturbations when a mixture fills the resonator requires a careful estimate of the thermal conductivity of the mixture. This property was obtained using the methods of kinetic theory reviewed by Giacobbe [14].

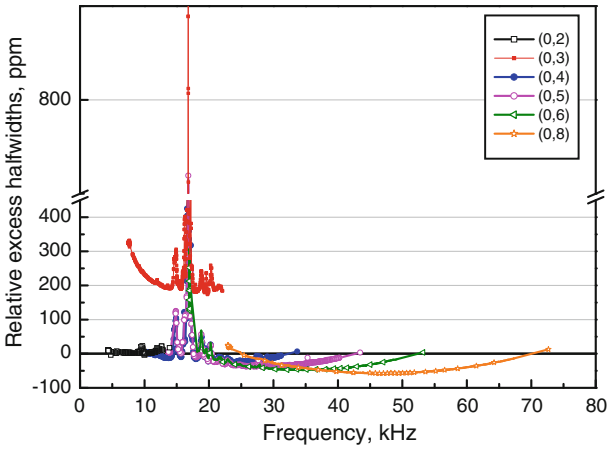


**Fig. 5** Overall recorded spectrum of TCU2v2, which shows the relative excess halfwidths of several radial modes in the frequency range between 4.4 kHz and 72.6 kHz

Besides the classical absorption caused by the irreversible flows of heat and momentum that are associated with sound propagation in pure gases, extra absorption takes place in a mixture due to mass and thermal diffusion effects, with a contribution to the halfwidths [15]:

$$g_{\mathrm{diff}} = \frac{\pi f^2}{u_{\mathrm{mix}}^2}\gamma_{\mathrm{mix}} x(1-x) D_{\mathrm{He-Ar}} \left( \frac{M_{\mathrm{Ar}} - M_{\mathrm{He}}}{M_{\mathrm{mix}}} + \frac{\gamma_{\mathrm{mix}} - 1}{\gamma_{\mathrm{mix}}} \alpha_{\mathrm{He-Ar}} \right)^2, \qquad (3)$$

where $u$ is the speed of sound, $\gamma$ is the heat-capacity ratio, $M$ is the molar mass, and $\alpha_{\mathrm{He-Ar}}$ and $D_{\mathrm{He-Ar}}$ are the thermal diffusion factor and the mutual diffusion coefficient, respectively, of helium and argon.

To evidence gas–shell coupling perturbations in the preparation of acoustic data, we did not apply any correction to take these effects into account. However, we used the model in [1] to calculate expected breathing frequencies for INRiM1 and TCU2v2 at 20.2 kHz and 19.3 kHz, respectively. The elastic and mechanical properties of steel and copper which are needed for these calculations are listed in Table 1 [10,16]. Using these properties, we construct Fig. 3 which compares the relative shell perturbations $\Delta f'_{\mathrm{shell}} = (f' - f_0)/f_0$ to the radial acoustic modes (0,2) to (0,10) expected in TCU2v2 when filled with Ar at 690 kPa, for two different constructing materials (steel or copper). Here, the material-dependent shift in the breathing frequency is mainly a consequence of the lower acoustic impedance of copper with respect to steel. While these kind of plots may, in principle, be helpful for the optimal design of an acoustic resonator, the direct measurement of the shell response shows significant deviations from this simple model. The relative excess halfwidths $\Delta g_{\mathrm{shell}} = (g_{\mathrm{exp}} - g_{\mathrm{calc}})/f_0$ and the relative frequency perturbations of the radial modes recorded for both INRiM1 (Fig. 4) and TCU2v2 (Fig. 6) in fact show the relevant effect of several other shell resonances in addition to that predicted by the analytical model. To prepare these plots, the predicted values $g_{\mathrm{calc}}$ were calculated as the sum of three contributions $g_{\mathrm{th}}$, $g_{\mathrm{bulk}}$, and

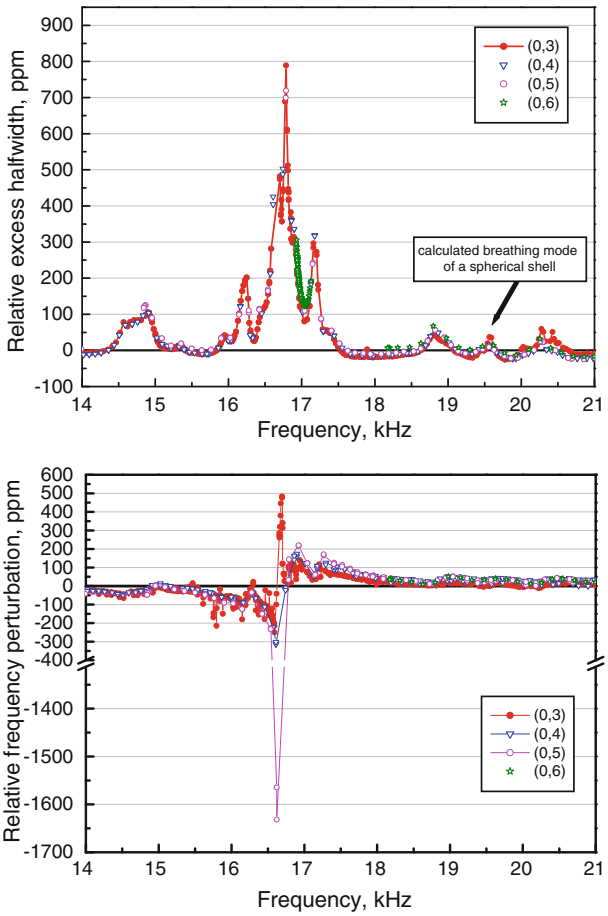


**Fig. 6** Relative excess halfwidths and frequency perturbations of radial modes recorded for the resonator TCU2v2

$g_{\text{diff}}$ from the thermal energy losses in the boundary layer, and the visco-thermal and diffusive losses taking place in the bulk of the gas, respectively. The latter term $g_{\text{diff}}$ was calculated using the values $D_{\text{He-Ar}} = 0.641 \times 10^{-4}\,\text{m}^2 \cdot \text{s}^{-1}$, and $\alpha_{\text{He-Ar}} = 0.38$ taken from the compilation by Chapman and Cowling [17].

Due to the rapid, continuous change of the composition of the gas sample, a simplified searching algorithm was employed to follow and bracket the position of the acoustic modes of interest. The imperfect functioning of this algorithm, and the need to speed up the acquisition process allowed recording of a complete set of data over the whole composition range ($1 > x > 0.5$) for modes (0,2) and (0,4) only. As a consequence, the INRiM1 data plotted in Fig. 4 for modes (0,3), (0,5), and (0,6) show some interruptions in their continuity. The numerical quantities plotted in the bottom graph in Fig. 4 were calculated as $10^6 \times (f_{0,n}^{\text{exp}}/f_{0,2}^{\text{exp}} - z_{0,n}/z_{0,2})$ assuming that the radial mode (0,2), which spans a lower frequency range while the composition of the

mixture is varied, is unaffected by relevant shell effects. Remarkably, the plots in Fig. 4 show that the shell perturbations do approximately affect the halfwidths of several different radial modes to the same relative extent. Also, a satisfactory correspondence is apparent in the location and the relevance of the shell perturbations as revealed by both the frequencies and the halfwidths of the investigated cavity resonances. At frequencies below 15 kHz and above 22 kHz, i.e., outside the frequency range displayed in Fig. 4, the excess halfwidths of the various radial modes investigated for INRiM1 over the range ($1 > x_{\mathrm{He}} > 0.5$) did not show evidence of any major perturbation. One single notable exception to this trend was observed for mode (0,2) which shows a pronounced peak at 8.5 kHz. This peak was not at all evident for the (0,3) mode, seemingly indicating that the perturbation to mode (0,2) was not induced by a shell effect.

The overall recorded spectrum of TCU2v2 in Fig. 5 shows the relative excess halfwidths of several radial modes spanning an overall frequency range between 4.4 kHz and 72.6 kHz. Here, the relevant shift in the halfwidth data for the mode (0,3) was later found to be caused by two annular ducts around the microwave straight probes. It should be noted that the perturbing effect of these holes is highly insensitive to the change of the speed of sound in the mixture, as expected from the constant proportion between the acoustic admittance of the cavity and the ducts. Thus, such features in the shell spectra may be used to correctly identify and distinguish between shell and duct effects. When the bias caused by the holes is subtracted from the (0,3) data, the detail of the most interesting part of the spectrum of TCU2v2 (Fig. 6) shows many features similar to those of INRiM1, with many convoluted local maxima which are found at a lower frequency than the predicted breathing mode. The plots in the lower part of Fig. 6 were calculated as $10^6 \times (f_{0,n}^{\mathrm{exp}}/f_{0,8}^{\mathrm{exp}} - z_{0,n}/z_{0,8})$ as the mode (0,8) spans a frequency range which is apparently (Fig. 5) not severely disturbed by the presence of shell perturbations.

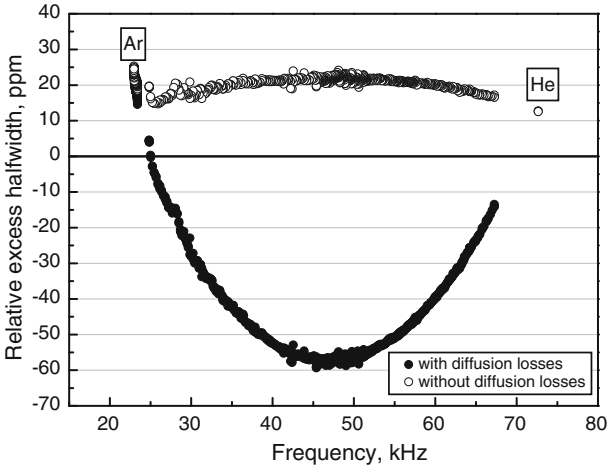


**Fig. 7** Effect of including the diffusion losses in the calculation of the halfwidth of mode (0,8) of TCU2v2 resonator

On both spectra showing the excess halfwidths of INRiM1 and TCU2v2 in Figs. 4 and 6, a relevant negative difference is observed in the baseline of the excess halfwidths, which away from the most effective shell perturbations would be expected to be null. This curved trend is more clearly shown in Fig. 7, which displays the difference in the excess halfwidths of mode (0,8) of TCU2v2, upon alternatively including or excluding the mixture diffusion term in Eq. 3. Speculating about a possible explanation for these discrepancies, it seems likely that it might be caused by the imperfect estimate of the diffusion coefficients in Eq. 3 or the other transport properties (thermal conductivity and viscosity) involved in the calculation of the energy losses associated with the acoustic propagation in the mixture. This observation suggests that the method proposed here to determine the shell spectrum and its effects on the eigenfrequencies of an acoustic resonator might also be useful for a revision of the transport properties of a binary mixture.

## References


1. J.B. Mehl, J. Acoust. Soc. Am. **78**, 782 (1985)
2. L. Pitre, M.R. Moldover, W.L. Tew, Metrologia **43**, 142 (2006)
3. G. Benedetto, R.M. Gavioso, R. Spagnolo, P. Marcarino, A. Merlone, Metrologia **41**, 74 (2004)
4. B. Fellmuth, C. Gaiser, J. Fischer, Meas. Sci. Technol. **17**, R145 (2006)
5. M.R. Moldover, C.R. Phys. **10**, 815 (2009)
6. J.B. Mehl, private communication
7. P. Gélat, N. Joly, M. de Podesta, G. Sutton, R. Underwood, J. Phys.: Conf. Ser. **195**, 012002 (2009)
8. D. Truong, private communication
9. M.R. Moldover, J.P.M. Trusler, T.J. Edwards, J.B. Mehl, R.S. Davis, J. Res. Natl. Inst. Stand. Technol. **93**, 85 (1988)
10. R.M. Gavioso, G. Benedetto, P.A.G. Albo, D.M. Ripa, A. Merlone, C. Guianvarc'h, F. Moro, R. Cuccaro, Metrologia **47**, 387 (2010)
11. J.W. Schmidt, M.R. Moldover, Int. J. Thermophys. **24**, 375 (2003)
12. J.W. Schmidt, R.M. Gavioso, E.F. May, M.R. Moldover, Phys. Rev. Lett. **98**, 254504 (2007)
13. C. Tegeler, R. Span, W. Wagner, J. Phys. Chem. Ref. Data **28**, 779 (1999)
14. F.W. Giacobbe, J. Acoust. Soc. Am. **96**, 3568 (1994)
15. M. Kohler, Ann. Phys. **127**, 41 (1949)
16. N.J. Simon, E.S. Drexler, R.P. Reed, *Properties of Copper and Copper Alloys at Cryogenic Temperatures, NIST Monograph 177* (U.S. Government Printing Office, Washington, DC, 1992)
17. S. Chapman, T.G. Cowling, *The Mathematical Theory of Non-Uniform Gases*, 3rd edn. (Cambridge University Press, Cambridge, 1970)